Multiple Controlled Synchronization for 3-Rotor Vibration Unit with Varying Payload

Alexander Fradkov*. Olga Tomchina**
Viktoria Galitskaya*. Dmitry Gorlatov******

** Institute of Problems of Mechanical Engineering, Russian Academy of Sciences, Saint Petersburg, Russia (Tel: 812-321-4410; e-mail: fradkov@mail.ru)*
*** Saint Petersburg State Polytechnical University, Saint Petersburg, Russia (e-mail: otomchina@mail.ru)*
**** Saint Petersburg State Polytechnical University, Saint Petersburg, Russia (e-mail: kvika86@mail.ru)*
***** Saint Petersburg State Polytechnical University, Saint Petersburg, Russia (e-mail: dprog@mail.ru)*

Abstract: Two PI-algorithms for multiple synchronization of 3-rotor vibration units are studied under conditions of varying payload and bounded controlling torque by computer simulation. It is shown that both algorithms are able to provide stable multiple synchronous mode when self-synchronization fails. The system performance is analyzed for different loading velocities, different payload masses and different control bounds.

Keywords: multiple synchronization, multi-rotor vibration unit, proportional-integral control algorithm.

1. INTRODUCTION

One of the main problems arising when design of modern vibration units is keeping stable synchronous operation mode in order to achieve maximum amplitude of the platform vibrations under changing operation conditions and maximum vibrotransportation velocity. An usual way of solving that problem is based on exploiting self-synchronization phenomenon discovered by I. I. Blekhman [Blekhman, 2000], [Blekhman, 2012] who proposed a unified view on synchronization. Significant results on stability study of synchronous mode for mechanical systems were obtained in [Gauthier and Micheau, 2008], [Pogromsky, Belykh and Nijmeijer, 2003], [Wu, Wang and Li, 2012], [Ulrichs, Mann and Parlitz, 2009], [Pena-Ramirez, Fey and Nijmeijer, 2012], [Wang, Zhao and Yao, 2012], [Czolczynski, Perlikowski and Stefanski, 2012]. The results of the above mentioned works require however that the plant model is known rather accurately.

However in some cases synchronization is not stable enough. It happens e.g. if one needs to provide the desired phase shifts or when multiple synchronization is needed. In such cases the controlled synchronization may help.

A systematic approach to controlled synchronization of vibration units based on speed-gradient control algorithms was proposed in [Andrievsky, Blekhman, Bortsov, et al 2001], [Blekhman, Fradkov, Tomchina and Bogdanov, 2002], [Tomchina and Kudryavtseva, 2005], [Fradkov, Andrievsky and Boykov, 2012]. Controlled synchronization provides additional opportunities, especially for vibrotransportation of materials. It may keep constant the ratio of average velocities and/or phases of vibroactuators. Multiple synchronous mode introduces an asymmetry into the system and gains efficiency of vibrotransportation, since it allows to avoid congestion at the system output. It is especially important for subtle technologies like transportation of powdered, wet and adhesive materials. In addition, presence of multiple rotation frequencies in the system allows technology equipment to perform transportation (with low frequency vibrations) and screening/separation of dry materials simultaneously. Unlike the simple synchronization modes which can arise spontaneously and remain as the parameters change in a small area, the multiple synchronization mode is sensitive to vibration unit parameter variations. Therefore a stable multiple synchronous mode can only be achieved by means of advanced control.

In this paper two algorithms for multiple synchronization of multi-rotor vibration unit are proposed. The design is based on the speed-gradient method [Fradkov, 2007] applied previously to control of different mechanical systems including vibration units [Andrievsky, Blekhman, Bortsov et al, 2001], [Blekhman, Fradkov, Tomchina and Bogdanov, 2002]. The performance of the proposed system is analyzed by computer simulation for model of the 3-rotor vibration set-up with varying payload.

2. APPROXIMATE MULTIPLE FREQUENCY AND PHASE SYNCHRONIZATION

Traditionally frequency synchronization is understood as coincidence of angular velocities of rotors $\omega_s = \omega_r$; $s, r = 1, \ldots, k$. More general case is the so called *multiple frequency synchronization* understood in the sense of the relation [Blekhman, 2000], [Fradkov, 2007]

$$\omega_i = n_i \cdot \omega^* \ (i = 1, \ldots, k) \tag{1}$$

for some integer n_i, where $\omega^* > 0$ is synchronous frequency.

In practice the notion of *approximate multiple frequency synchronization* may be of use:

$$\left| \omega_s - \frac{n_s}{n_r} \cdot \omega_r \right| \le \varepsilon. \tag{2}$$

Here $\varepsilon > 0$ can be chosen as $\varepsilon = 0.05\,\omega^*$, similarly to conventional definition of the transient time. However the relation (2) itself is not sufficient for synchronization since it admits accumulation of the multiple phase error. Therefore some additional restrictions with respect to the phases should be imposed.

Recall that the coordinate synchronization well studied in physics and mechanics [Blekhman, 2000], [Fradkov, 2007] arises when the outputs or some generalized coordinated of the subsystem coincide with the corresponding coordinates of other subsystems for all $t \ge t_0$. Similarly, the notion *of multiple coordinate synchronization* assumes that the phases φ_i, $i = 1, \ldots, k$ satisfy identities

$$\frac{\varphi_s}{n_s} - \frac{\varphi_r}{n_r} = L_{sr}; \quad s, r = 1, \ldots, k. \tag{3}$$

In practice the relation (3) cannot fulfill exactly and should be replaced by an approximate one:

$$\left| \frac{\varphi_s}{n_s} - \frac{\varphi_r}{n_r} - L_{sr} \right| < \varepsilon; \quad s, r = 1, \ldots, k. \tag{4}$$

Having that in mind *approximate multiple frequency and phase synchronization* is defined as fulfillment of the inequalities (2) and (4) for some $\varepsilon > 0$, $L_{sr} > 0$.

3. CONTROL ALGORITHM FOR MULTIPLE SYNCHRONIZATION

First of all let us introduce the idea of Speed-Gradient (SG) algorithm, following [Andrievsky, Blekhman, Bortsov, *et al* 2001], [Fradkov, 2007]. Let the controlled system dynamics be described by the state space differential equations

$$dz / dt = F(z, M), \tag{5}$$

where z is n-dimensional state vector (e.g. for mechanical systems described by Lagrange 2nd kind equations z consists of generalized coordinates and their derivatives); M is the vector of controlling variables (torques). Let the control goal be described by the nonnegative goal function (GF) $Q(z) \ge 0$:

$$Q(z(t)) \to 0 \ \textit{as} \ t \to \infty. \tag{6}$$

Then the speed-gradient control algorithm is as follows:

$$M = -\gamma \nabla_M \dot{Q}(z), \tag{7}$$

where notation $\dot{Q}(z) = \dfrac{dQ(z)}{dt}$ stands for the time derivative of GF along trajectories of the controlled system, ∇ – symbol of gradient (vector of partial derivatives), γ is gain.

To apply speed-gradient method one needs to choose the goal function, evaluate its speed of its change along trajectories of controlled system and to change control in the direction of the gradient of the evaluated speed. The first suggestion is to choose the goal function as follows:

$$Q(z) = \left\{ 0.5(1-\alpha)(H - H^*)^2 + \sum_{s,r \ne s}^{k} \alpha_{s,r} (\dot{\varphi}_s / n_s \pm \dot{\varphi}_r / n_r)^2 \right\}, \tag{8}$$

where z is the state vector of the system; $\dot{\varphi}_i$ are angular velocities of unbalanced rotors (vibroactuators), $\alpha_{s,r} > 0$, $\sum_{s,r>s}^{k} \alpha_{s,r} = \alpha$, $0 < \alpha < 1$ are weighting coefficients; H is the total mechanical energy, H^* is the desired level of H. Obviously the goal is achieved if $Q(z) = 0$, otherwise $Q(z) > 0$. If $Q(z) = 0$ then $H = H^*$, it provides required rotor velocities and multiple synchronization relation $\dot{\varphi}_s / n_s = \pm \dot{\varphi}_r / n_r$. Note that at the first stage of design the friction has been neglected. Applying the speed-gradient method the speed of changing (8) along trajectories of controlled system and the gradient of the speed with respect to controlling variables (torques) are evaluated. Then the designed control algorithm is as follows:

$$M_s = \gamma_s \left\{ (1-\alpha)(H - H^*) \dot{\varphi}_s \pm \sum_r \alpha_{sr} (\dot{\varphi}_s / n_s \pm \dot{\varphi}_r / n_r) \right\}, \tag{9}$$

where M_s are controlling torques, $\gamma_s > 0$ are control gains, $s = 1,\ldots,k$. The control algorithm (9) is called the *mutual synchronization algorithm*.

A different approach is based on the goal function

$$Q(z) = 0.5 \left\{ (1-\alpha)(H - H^*)^2 + \sum_{r>1}^{k} \alpha_{1,r} (\dot{\varphi}_1 / n_1 \pm \dot{\varphi}_r / n_r)^2 \right\}. \tag{10}$$

Applying the speed-gradient method, the following control algorithm is designed:

$$M_s = -\gamma_s \left\{ (1-\alpha)(H - H^*) \dot{\varphi}_s \pm \sum_r \alpha_{1,r} (\dot{\varphi}_1 / n_s \pm \dot{\varphi}_r / n_r) \right\}. \tag{11}$$

Here the rotors indexed with the numbers $r = 2, \ldots, k$ are pushed to synchronize with the first rotor. The control algorithm (11) is called the *synchronization algorithm with the leading rotor*.

More general form of SG-algorithm is [Fradkov (1986)]:

$$M = -\frac{\beta + \gamma p}{\delta + p} \nabla_M \Psi(z), \tag{12}$$

where $p = d / dt$ is operator of differentiation in time, β, γ, δ are nonnegative coefficients, $\Psi(z) = \dot{Q}(z)$.

4. VIBRATION UNIT DYNAMICS

Efficiency of the proposed algorithms was analyzed for 3-rotor vibration unit [Andrievsky, Blekhman, Bortsov, *et al* 2001] model with 6 degrees of freedom taking into account 3 degrees of freedom for supporting body (Fig. 1).

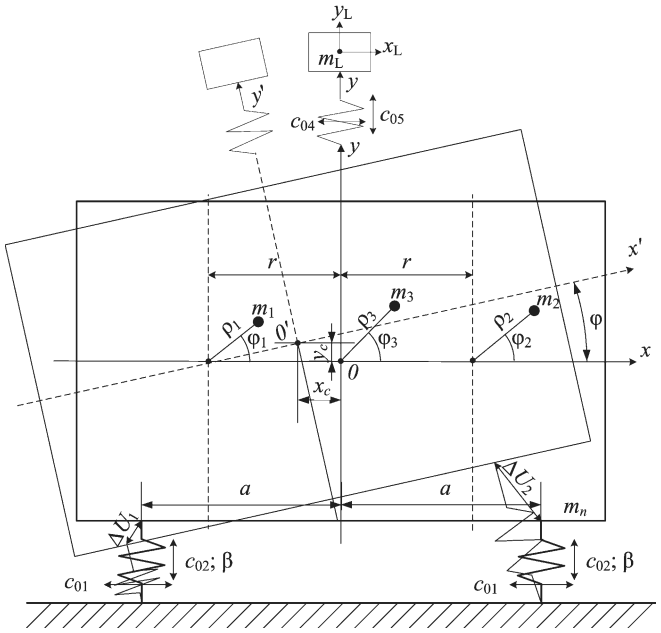

Fig. 1. The kinematic scheme of controlled mechanical system with payload.

Here φ_1, φ_2, φ_3 are rotation angles of the rotors measured from the horizontal position, x_c, y_c are the horizontal and vertical displacement of the supporting body from the equilibrium position, $m_i = m$, are the masses of the rotors, J_1, J_2, J_3 are the inertia moments of the rotors, $\rho_i = \rho$ is the eccentricity of rotors, c_{01}, c_{02} are the horizontal and vertical spring stiffness, g is the gravitational acceleration, m_0 is the total mass of the unit, β is the damping coefficient, k_c the friction coefficient in the bearings, M_1, M_2, M_3 are the motor torques (controlling variables); x_L, y_L are coordinates of the payload center of the mass in the rest frame. The motion of the rotor shafts is supposed orthogonal to the support movement.

The unit dynamics can be described by the Lagrange second kind equations

$$
\begin{aligned}
&m_0\ddot{y}_c + \ddot{\varphi}m\rho(\cos(\varphi+\varphi_1)+\cos(\varphi+\varphi_2)+\cos(\varphi+\varphi_3)) - \\
&\ddot{\varphi}_1 m\rho\cos(\varphi+\varphi_1) - \ddot{\varphi}_2 m\rho\cos(\varphi+\varphi_2) - \ddot{\varphi}_3 m\rho\cos(\varphi+\varphi_3) - \\
&\dot{\varphi}^2 m\rho(\sin(\varphi+\varphi_1)+\sin(\varphi+\varphi_2)+\sin(\varphi+\varphi_3)) - \\
&\dot{\varphi}_1^2 m\rho\sin(\varphi+\varphi_1) - \dot{\varphi}_2^2 m\rho c\sin(\varphi+\varphi_2) - \dot{\varphi}_3^2 m\rho\sin(\varphi+\varphi_3) - \\
&2\dot{\varphi}\dot{\varphi}_1 m\rho\sin(\varphi+\varphi_1) - 2\dot{\varphi}\dot{\varphi}_2 m\rho\sin(\varphi+\varphi_2) - \\
&2\dot{\varphi}\dot{\varphi}_3 m\rho\sin(\varphi+\varphi_3) + m_0 g + 2c_{02}y_c + \beta\dot{y}_c + c_{05}(y_c - y_L) = 0;
\end{aligned}
$$

$$
\begin{aligned}
&-\ddot{x}_c m\rho(\sin(\varphi+\varphi_1)+\sin(\varphi+\varphi_2)+\sin(\varphi+\varphi_3)) + \\
&\ddot{y}_c m\rho(\cos(\varphi+\varphi_1)+\cos(\varphi+\varphi_2)+\cos(\varphi+\varphi_3)) + \\
&\ddot{\varphi}\big(J + J_1 + J_2 + J_3 - 2rm\rho(\cos\varphi_1 - \cos\varphi_2)\big) + \\
&\ddot{\varphi}_1(J_1 - rm\rho\cos\varphi_1) + \ddot{\varphi}_2(J_2 + rm\rho\cos\varphi_2) + \ddot{\varphi}_3 J_3 + \\
&\dot{\varphi}_1^2 rm\rho\sin\varphi_1 - \dot{\varphi}_2^2 rm\rho\sin\varphi_2 + 2rm\rho\dot{\varphi}\dot{\varphi}_1\sin\varphi_1 - \\
&2rm\rho\dot{\varphi}\dot{\varphi}_2\sin\varphi_2 + m\rho g(\cos(\varphi+\varphi_1)+\cos(\varphi+\varphi_2)+ \\
&+\cos(\varphi+\varphi_3)) + c_{03}\varphi + \beta\dot{\varphi} = 0;
\end{aligned}
\tag{13}
$$

$$
\begin{aligned}
&-\ddot{x}_c m\rho\sin(\varphi+\varphi_1) + \ddot{y}_c m\rho\cos(\varphi+\varphi_1) + \ddot{\varphi}(J_1 - rm\rho\cos\varphi_1) + \\
&\ddot{\varphi}_1 J_1 - \dot{\varphi}^2 rm\rho\sin\varphi_1 + m\rho g\cos(\varphi+\varphi_1) + k_c\dot{\varphi}_1 = M_1;
\end{aligned}
$$

$$
\begin{aligned}
&-\ddot{x}_c m\rho\sin(\varphi+\varphi_2) + \ddot{y}_c m\rho\cos(\varphi+\varphi_2) + \ddot{\varphi}(J_2 + rm\rho\cos\varphi_1) + \\
&\ddot{\varphi}_2 J_2 + \dot{\varphi}^2 rm\rho\sin\varphi_2 + m\rho g\cos(\varphi+\varphi_2) + k_c\dot{\varphi}_2 = M_2;
\end{aligned}
$$

$$
\begin{aligned}
&-\ddot{x}_c m\rho\sin(\varphi+\varphi_3) + \ddot{y}_c m\rho\cos(\varphi+\varphi_3) + \\
&\ddot{\varphi}J_3 + \ddot{\varphi}_3 J_3 + m\rho g\cos(\varphi+\varphi_3) + k_c\dot{\varphi}_3 = M_3;
\end{aligned}
$$

$$m_L\ddot{x}_L - c_{04}(x_c - x_L) + \beta\dot{x}_L + m_L\dot{x}_L = 0;$$

$$m_L\ddot{y}_L - c_{05}(y_c - y_L) + \beta\dot{y}_L + m_L\dot{y}_L + m_L g = 0.$$

Kinetic and potential energies T and Π are as follows:

$$
\begin{aligned}
&T = 0.5m_0(\dot{x}_c^2 + \dot{y}_c^2) + 0.5m_L(\dot{x}_L^2 + \dot{y}_L^2) + \\
&0.5\dot{\varphi}^2(J + J_1 + J_2 + J_3 - 2rm\rho(\cos\varphi_1 - \cos\varphi_2)) + \\
&0.5J_1\dot{\varphi}_1^2 + 0.5J_2\dot{\varphi}_2^2 + 0.5J_3\dot{\varphi}_3^2 + \\
&\dot{\varphi}\dot{\varphi}_1(J_1 - dm\rho\cos\varphi_1) + \dot{\varphi}\dot{\varphi}_2(J_2 + dm\rho\cos\varphi_2) + \\
&\dot{\varphi}\dot{\varphi}_3 J_3 - \dot{x}_c\dot{\varphi}m\rho(\sin(\varphi+\varphi_1)+\sin(\varphi+\varphi_2)+\sin(\varphi+\varphi_3)) + \\
&\dot{y}_c\dot{\varphi}m\rho(\cos(\varphi+\varphi_1)+\cos(\varphi+\varphi_2)+\cos(\varphi+\varphi_3)) - \\
&\dot{x}_c\dot{\varphi}_1 m\rho\sin(\varphi+\varphi_1) + \dot{y}_c\dot{\varphi}_1 m\rho\cos(\varphi+\varphi_1) - \\
&\dot{x}_c\dot{\varphi}_2 m\rho\sin(\varphi+\varphi_2) + \dot{y}_c\dot{\varphi}_2 m\rho\cos(\varphi+\varphi_2) - \\
&\dot{x}_c\dot{\varphi}_3 m\rho\sin(\varphi+\varphi_3) + \dot{y}_c\dot{\varphi}_3 m\rho\cos(\varphi+\varphi_3),
\end{aligned}
$$

$$
\begin{aligned}
&\Pi = (m_n + 3m)gy_c + m_L g y_L + m\rho g(\sin(\varphi+\varphi_1) + \\
&+\sin(\varphi+\varphi_2)+\sin(\varphi+\varphi_3)) + c_{01}(x_c^2 + a^2\cos^2\varphi)^2 + \\
&c_{02}(y_c^2 + a^2\sin^2\varphi)^2 + 0.5c_{04}(x_c - x_L)^2 + 0.5c_{05}(y_c - y_L)^2,
\end{aligned}
\tag{14}
$$

$$H = T + \Pi.$$

5. SIMULATION RESULTS

Simulation was performed in MATLAB environment. Simulation results for 3-rotor vibration unit (13) with conventional control ($M_i = const$) are presented in Fig. 2 - Fig. 3. To create double-synchronous mode with parameters $n_1 = n_2 = 1$, $n_3 = 2$ the torque values were chosen as follows: $M_1 = M_2 = 2$ *N·m*, $M_3 = 4$ *N·m*. It corresponds to the following rotor velocities: $\dot{\varphi}_1 = \dot{\varphi}_2 = 200s^{-1}$, $\dot{\varphi}_3 = 400s^{-1}$. The simulation results show multiple self-synchronization failure. Namely the values of multiple phase shifts are not stabilized: $\varphi_i - \varphi_3/2 \to \infty$, i=1,2, (Fig. 2) and multiple velocity differences is not preserved (Fig. 3).

In Fig. 2, 3 the plots for double self-synchronization mode for 3-rotor vibration unit with $M_1 = M_2 = 2$ *N·m*, $M_3 = 4$ *N·m*.

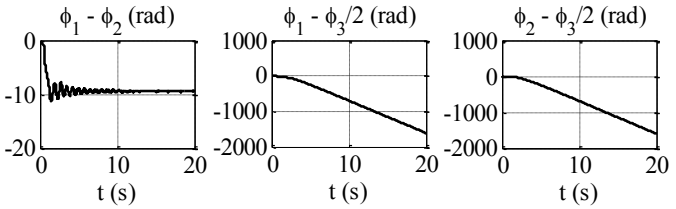

Fig. 2. The plots of the multiple velocity differences.

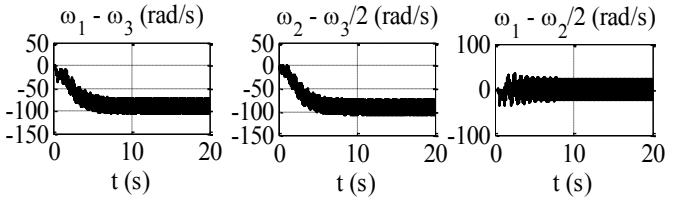

Fig. 3. The plots of the multiple phase shifts.

It is seen from the plots of the multiple velocity differences and the multiple phase shift (Fig. 2, Fig. 3) that the multiple self-synchronization is established:

$$\varphi_i / n_i - \varphi_j / n_j \to \text{const}; \quad \Delta\dot{\varphi} = (\dot{\varphi}_i / n_i - \dot{\varphi}_j / n_j) \to 0. \quad (15)$$

To ensure the stable multiple synchronization of three rotors in a 3-rotor vibrational unit two control algorithms are specified from (9), (11). The first algorithm is based upon the functional (8) where all pairs of velocity differences are taken into account. The algorithm looks as follows:

$$Q(z) = 0.5\left\{(1-\alpha)(H-H^*)^2 + \alpha_{12}\left(\frac{\dot{\varphi}_1}{n_1} \pm \frac{\dot{\varphi}_2}{n_2}\right)^2 + \alpha_{13}\left(\frac{\dot{\varphi}_1}{n_1} \pm \frac{\dot{\varphi}_3}{n_3}\right)^2 + \alpha_{23}\left(\frac{\dot{\varphi}_2}{n_2} \pm \frac{\dot{\varphi}_3}{n_3}\right)^2\right\}. \quad (16)$$

According to the SG-scheme, setting $\delta = 0$ in (12), the proportional-integral (PI) control algorithm is proposed [Fradkov et al., 2013] (note that for in-phase synchronization the sign «-» should be chosen in (10)).

$$\begin{cases} \tilde{M}_1 = -\gamma_1\left\{(1-\alpha)(\tilde{H}-H^*)\dot{\varphi}_1 + \frac{\alpha_{12}}{J_1 n_1}\left(\frac{\dot{\varphi}_1}{n_1} - \frac{\dot{\varphi}_2}{n_2}\right) + \right. \\ \left. \frac{\alpha_{13}}{J_1 n_1}\left(\frac{\dot{\varphi}_1}{n_1} - \frac{\dot{\varphi}_3}{n_3}\right) + \frac{\alpha_{12}}{J_1 n_1}\left(\frac{\varphi_1}{n_1} - \frac{\varphi_2}{n_2}\right) + \frac{\alpha_{13}}{J_1 n_1}\left(\frac{\varphi_1}{n_1} - \frac{\varphi_3}{n_3}\right)\right\}; \\ \tilde{M}_2 = -\gamma_2\left\{(1-\alpha)(\tilde{H}-H^*)\dot{\varphi}_2 - \frac{\alpha_{12}}{J_2 n_2}\left(\frac{\dot{\varphi}_1}{n_1} - \frac{\dot{\varphi}_2}{n_2}\right) + \right. \\ \left. \frac{\alpha_{23}}{J_2 n_2}\left(\frac{\dot{\varphi}_2}{n_2} - \frac{\dot{\varphi}_3}{n_3}\right) - \frac{\alpha_{12}}{J_2 n_2}\left(\frac{\varphi_1}{n_1} - \frac{\varphi_2}{n_2}\right) + \frac{\alpha_{23}}{J_2 n_2}\left(\frac{\varphi_2}{n_2} - \frac{\varphi_3}{n_3}\right)\right\}; \\ \tilde{M}_3 = -\gamma_3\left\{(1-\alpha)(\tilde{H}-H^*)\dot{\varphi}_3 - \frac{\alpha_{13}}{J_3 n_3}\left(\frac{\dot{\varphi}_1}{n_1} - \frac{\dot{\varphi}_3}{n_3}\right) - \right. \\ \left. \frac{\alpha_{23}}{J_3 n_3}\left(\frac{\dot{\varphi}_2}{n_2} - \frac{\dot{\varphi}_3}{n_3}\right) - \frac{\alpha_{13}}{J_3 n_3}\left(\frac{\varphi_1}{n_1} - \frac{\varphi_3}{n_3}\right) - \frac{\alpha_{23}}{J_3 n_3}\left(\frac{\varphi_2}{n_2} - \frac{\varphi_3}{n_3}\right)\right\}. \end{cases} \quad (17)$$

The second control algorithm based upon the functional (10) is as follows:

$$Q(z) = 0.5\left\{(1-\alpha)(H-H^*)^2 + \alpha_{12}\left(\frac{\dot{\varphi}_1}{n_1} \pm \frac{\dot{\varphi}_2}{n_2}\right)^2 + \alpha_{13}\left(\frac{\dot{\varphi}_1}{n_1} \pm \frac{\dot{\varphi}_3}{n_3}\right)^2\right\}. \quad (18)$$

$$\begin{cases} \tilde{M}_1 = -\gamma_1\left\{(1-\alpha)(\tilde{H}-H^*)\dot{\varphi}_1 + \frac{\alpha_{12}}{J_1 n_1}\left(\frac{\dot{\varphi}_1}{n_1} - \frac{\dot{\varphi}_2}{n_2}\right) + \right. \\ \left. \frac{\alpha_{13}}{J_1 n_1}\left(\frac{\dot{\varphi}_1}{n_1} - \frac{\dot{\varphi}_3}{n_3}\right) + \frac{\alpha_{12}}{J_1 n_1}\left(\frac{\varphi_1}{n_1} - \frac{\varphi_2}{n_2}\right) + \frac{\alpha_{13}}{J_1 n_1}\left(\frac{\varphi_1}{n_1} - \frac{\varphi_3}{n_3}\right)\right\}; \\ \tilde{M}_2 = -\gamma_2\left\{(1-\alpha)(\tilde{H}-H^*)\dot{\varphi}_2 - \frac{\alpha_{12}}{J_2 n_2}\left(\frac{\varphi_1}{n_1} - \frac{\varphi_2}{n_2}\right) - \right. \\ \left. \frac{\alpha_{12}}{J_2 n_2}\left(\frac{\varphi_1}{n_1} - \frac{\varphi_2}{n_2}\right)\right\}; \\ \tilde{M}_3 = -\gamma_3\left\{(1-\alpha)(\tilde{H}-H^*)\dot{\varphi}_3 - \frac{\alpha_{13}}{J_3 n_3}\left(\frac{\dot{\varphi}_1}{n_1} - \frac{\dot{\varphi}_3}{n_3}\right) - \right. \\ \left. \frac{\alpha_{13}}{J_3 n_3}\left(\frac{\varphi_1}{n_1} - \frac{\varphi_3}{n_3}\right)\right\}. \end{cases} \quad (19)$$

where $\tilde{H}$ is the reduced expression for the total energy of the system. Having in mind that SG-algorithms possess some degree of robustness the expression of total mechanical energy is simplified with the aim of simplifying the controller. To this end it is worth noting that the value of the angle φ is typically small in the steady state mode: $|\varphi| \le 1.8°$. Therefore the expression for total energy is simplified letting $\varphi = 0$. In addition the terms corresponding to the payload energy are dropped since its mass is uncertain and cannot be measured. Then the reduced energy to be used in the reduced algorithm is as follows:

$$\begin{aligned} \tilde{H} = {} & 0.5 m_0 \dot{x}_c^2 + 0.5 m_0 \dot{y}_c^2 + 0.5 J_1 \dot{\varphi}_1^2 + 0.5 J_2 \dot{\varphi}_2^2 + 0.5 J_3 \dot{\varphi}_3^2 - \\ & \dot{x}_c \dot{\varphi}_1 m\rho \sin\varphi_1 + \dot{y}_c \dot{\varphi}_1 m\rho \cos + \varphi_1 - \dot{x}_c \dot{\varphi}_2 m\rho \sin\varphi_2 + \\ & \dot{y}_c \dot{\varphi}_2 m\rho \cos\varphi_2 - \dot{x}_c \dot{\varphi}_3 m\rho \sin\varphi_3 + \dot{y}_c \dot{\varphi}_3 m\rho \cos\varphi_3 + \\ & m_0 g y_c + m\rho g(\sin\varphi_1 + \sin\varphi_2 + \sin\varphi_3) + c_{01}(x_c^2 + a^2) + c_{02} y_c^2. \end{aligned} \quad (20)$$

Justification of the algorithm is made by computer simulation. Application of the algorithm with one leading rotor (17) ensures the desired multiple synchronous mode (n_1=n_2=1, n_3=2) not only under conditions of the previous experiment yet for varying payload too. The results presented in Fig. 4 and Fig. 5 correspond to the case $m_L(0)$=1 kg and loading rate V=2 *kg/s*. It corresponds to the deviation of the payload mass $\Delta m_L = 0.5 m_0$, that is typical for vibration screens. The linear loading law $\Delta m_L = m_L(0) + Vt$ is applied, $t_1 \le t \le t_2$. In simulation the loading rate was varied from 1 *kg/s* to 12 *kg/s* providing $\Delta m_L = V(t_1 - t_2) = 0.5 m_0$. In Fig. 4 the multiple velocity plots are presented: $\dot{\varphi}_i = \dot{\varphi}_3 / 2$, i=1,2, with the average values $\dot{\varphi}_{1,2} = 100 s^{-1}$, $\dot{\varphi}_3 = 200 s^{-1}$. In Fig. 5 the values of multiple phase shifts $\varphi_i / n_i - \varphi_j / n_j$, i, j=1,2,3 are shown. It is seen that the values of multiple phase shifts are stabilized that is indicates existence of the approximate multiple synchronous mode. After loading the oscillations of the support have stable amplitude in both horizontal and vertical directions (Fig. 6).

Note that many conventional control algorithms such as modal controller or model reference adaptive controller generate control signals far exceeding admitted values in the startup mode. Therefore saturation is often inserted into the controller system.

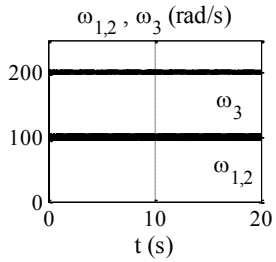

Fig. 4. The multiple velocity plots.

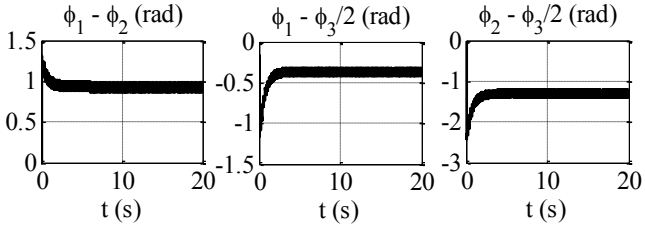

Fig. 5. The multiple phase shifts.

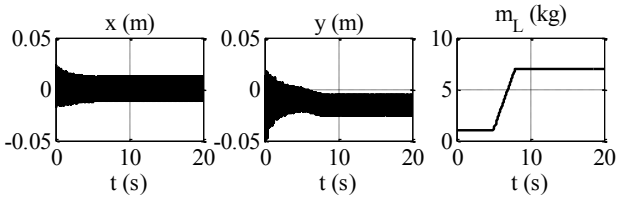

Fig. 6. The amplitudes of the oscillations of the support in horizontal and vertical directions and payload variation plot.

Simulation results for 3-rotor vibration unit (13) and controller with one leading rotor and saturation are presented in Fig. 7. Simulations were carried out for H^*=300 J, V=3 kg/s, t_1=10 s, t_2=12 s. They demonstrate satisfactory performance of the closed loop system. In Fig. 8 the plot of controlling torque M_1 under constraint $|M_i|<6$ $N{\cdot}m$ is presented. Note that maximum value of M_1 in the unconstrained system for the same parameters is M_1=82 $N{\cdot}m$.

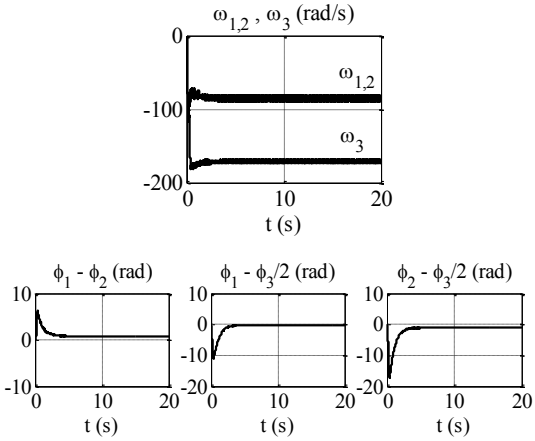

Fig. 7. The multiple velocity and multiple phase shifts plots.

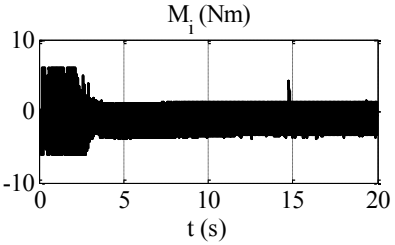

Fig. 8. The plot of controlling torque M_1.

Analysis was performed in the above-resonance frequency zone for in the range $\dot{\varphi}_i \in [\omega_p, \dot{\varphi}^*_{\min}]$, where ω_p=30 s^{-1} is resonance frequency, $\dot{\varphi}^*_{\min} = 300\ s^{-1}$ are minimum rotor velocities, achievable with constant torques. Presence of the time-varying elastically connected payload does not destroy synchronization both for algorithm (17), and for (15). Moreover, synchronization time almost does not depend on loading rate and the final value of the payload mass. It is mainly specified by the desired energy value H^*, which in turn determines the steady-state rotor velocities $\dot{\varphi}_i(\infty)$. Besides, the closer $\dot{\varphi}_i(\infty)$ to resonance frequency the larger is synchronization time.

The nomograms for dependence of synchronization time of the value of H^* are shown in Fig. 9 and Fig. 10 for simple (n_i=1) and double (n_1=n_2=1, n_3=2) synchronous mode in the system without and with restriction imposed on the control signal level. Note that the level of the constraint is of the order of constant work torques for conventional control. It allows one to use algorithms (15) and (17) for real vibration units.

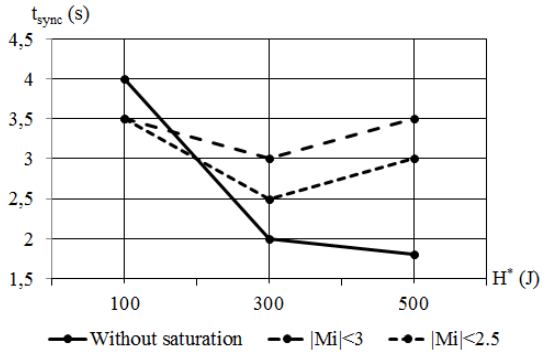

Fig. 9. Nomogram for dependence of synchronization time of the value of H^* (n_i=1).

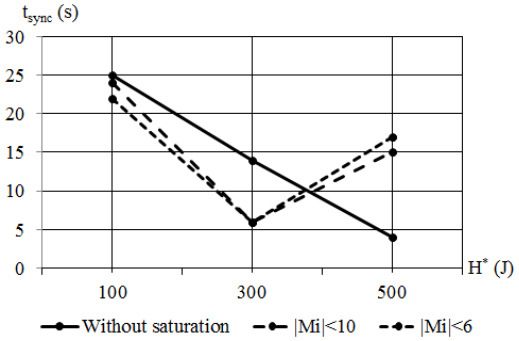

Fig. 10. Nomogram for dependence of synchronization time of the value of H^* (n_1=n_2=1, n_3=2).

6. CONCLUSIONS

The main contribution of our study is design and comparison of two control algorithms providing stable multiple synchronous mode in multi-rotor vibration units with different multiplicities. It is confirmed by numerous simulation results, some of them are presented in the paper. Note that some design and simulation results for the first algorithm were presented in [Galitskaya, Tomchina, 2012].

The work was supported by Russian Foundation for Basic Research (grant 11-08-01218) and Research Program N. 10 of OEMMPU Division of RAS.

Obviously, in terms of implementation, algorithm (17) is simpler. However algorithm (15) also has some benefits. For example, algorithm (15) allows us to narrow the after-resonance zone of speeds unreachable for running at synchronous mode. For large values of $\dot{\varphi}_i(\infty)$ the results for both algorithms are practically identical.

REFERENCES

Andrievsky B.R., Blekhman I.I., Bortsov Yu.A., Fradkov A.L., Gavrilov S.V., Konoplev V.A., Lavrov B.P., Polyakhov N.D., Shestakov V.M., Tomchina O.P. (2001). *Control of mechatronic vibration units* / Eds. Blekhman I.I., Fradkov A.L. Nauka, St.Petersburg, (in Russian).

Blekhman I.I. (2000). *Vibrational mechanics*. Singapore: World Scientific, 510 p.

Blekhman I.I. (2012). Oscillatory strobodynamics— a new area in nonlinear oscillations theory, nonlinear dynamics and cybernetical physics. *Cybernetics and Physics*, V.1, Is.1, pp. 5-10.

Blekhman I.I., Fradkov A.L., Tomchina O.P., Bogdanov D.E. (2002). Self-Synchronization and Controlled Synchronization: General Definition and Example Design. *Mathematics and Computers in Simulation*, V.58, Is. 4-6, pp. 367-384.

Czolczynski K., Perlikowski P., Stefanski, A., et al. (2012). Synchronization of slowly rotating pendulums. *International Journal Of Bifurcation And Chaos*, V. 22 Is. 5, 1250128.

Fradkov A.L., Andrievsky B., Boykov K.B. (2012). Multipendulum mechatronic setup: Design and experiments. *Mechatronics*, V. 22, pp. 76-82.

Fradkov A.L. (2007). *Cybernetical physics: from control of chaos to quantum control*. Springer-Verlag.

Fradkov A.L, Tomchina O.P, Galitskaya V.A., Gorlatov D.V. (2013) Integrodifferentiating speed-gradient algorithms for multiple synchronization of vibration units. Nauchno-tekhnicheskii Vestnik of ITMO, St.Petersburg, No1, pp. 30-37.

Galitskaya V.A., Tomchina O.P (2012). Proportional-integral energy-velocity algorithm for multiple synchronization control of vibration unit rotors. *Informatics and Control Systems*, V. 33, No 3, pp. 158-168.

Gauthier J.-P., Micheau P. Extremal harmonic active control of power for rotating machines (2008). *Journal of Sound And Vibration*, V. 318, Is. 4-5, pp. 663-677.

Pena-Ramirez J.,Fey R., Nijmeijer H. (2012). In-phase and anti-phase synchronization of oscillators with Huygens' coupling. *Cybernetics and Physics*, V.1, Is.1, pp. 58-66.

Pogromsky A.Yu, Belykh V.N., Nijmeijer H. (2003). Controlled synchronization of pendula. *Proc. 42nd IEEE Conference On Decision And Control*, pp. 4381-4386.

Tomchina O.P, Galitskaya V.A., Fradkov A.L. (2011). Algorithm of multiple synchronization for multi-rotor vibration unit. *7th European Nonlinear Dynamics Conference (ENOC 2011)*, Rome.

Tomchina O.P., Kudryavtseva I.M. (2005). Controlled synchronization of unbalanced rotors with flexible shafts in time-varying vibrational units. *Proc. 2nd Int.Conf. "Physics and Control"*, St.Petersburg, pp. 790-794.

Ulrichs H., Mann A., Parlitz U. (2009). Synchronization and chaotic dynamics of coupled mechanical metronomes. *CHAOS*, V. 19 Is. 4, Art. No.: 043120.

Wang D, Zhao C., Yao H. et al. (2012). Vibration Synchronization of a Vibrating System Driven by Two Motors. *Advances In Vibration Engineering*, V. 11 Is. 1, pp. 59-73.

Wu Y., Wang N., Li L. et al. (2012). Anti-phase synchronization of two coupled mechanical metronomes. *CHAOS*, V. 22, Is. 2, Art. No. 023146.